

MESON PRODUCTION OBSERVED WITH THE FOPI DETECTOR *

D. PELTE

Physikalisches Institut der Universität Heidelberg, Philosophenweg 12
D-69120 Heidelberg, Germany
The FOPI Collaboration
Gesellschaft für Schwerionenforschung mbH, Postfach 110552
D-64220 Darmstadt, Germany

(Received October 9, 1996)

Charged pion production is studied at different energies in two systems, Ni + Ni and Au + Au, using the FOPI detector at GSI. The pion production probability is found to be reduced for the heavier system. The rescattering of pions from spectator matter is observed under all conditions, it is responsible for the non-thermal shape of the rapidity spectra. The excited Baryon resonances are shown to be a major source of the observed pions, higher resonances than the $\Delta(1232)$ are responsible for pions with large transverse momenta.

PACS numbers: 13.60. Le

1. Introduction

The production of charged pions π^\pm was studied at bombarding energies ranging from 1 to 2 AGeV with the 4π detector FOPI at the SIS accelerator of the GSI/Darmstadt. The following symmetric projectile - target systems were measured:

- Au 1: $^{197}\text{Au} + ^{197}\text{Au}$ at $E = 1.06$ AGeV,
- Ni 1: $^{58}\text{Ni} + ^{58}\text{Ni}$ at $E = 1.06$ AGeV,
- Ni 2: $^{58}\text{Ni} + ^{58}\text{Ni}$ at $E = 1.45$ AGeV,
- Ni 3: $^{58}\text{Ni} + ^{58}\text{Ni}$ at $E = 1.93$ AGeV.

At the time of these experiments the FOPI detector was not yet completed. It consisted of the forward detectors PLA and ZER, which covered the lab. region from $1.2^\circ < \vartheta < 30^\circ$ with full azimuthal coverage, and of the central drift chamber CDC at angles $30^\circ < \vartheta < 150^\circ$, which was installed inside a

* Presented at the "Meson 96" Workshop, Cracow, Poland, May 10-14, 1996.

solenoidal magnet field of 0.6 T strength. Also the CDC provided full azimuthal coverage. Charged pions could only be identified in the CDC since the PLA and ZER detectors only allow nuclear charge identification.

Because of the CDC boundary at $\vartheta = 30^\circ$ only 30% of the pion phase space in the forward hemisphere of the cm frame was measured. To extent the coverage of the total phase space to approximately 90% the symmetry relation $f(\Theta, \Phi) = f(\pi - \Theta, \pi + \Phi)$ was employed which holds when target and projectile are identical.

To present the data we use a rapidity normalized to the cm rapidity

$$Y^{(0)} = (y - y_{\text{cm}})/y_{\text{cm}},$$

and a normalized transverse momentum

$$p_t^{(0)} = p_t/A \cdot (P_{\text{proj}}/A_{\text{proj}})^{-1}.$$

In general quantities in the cm frame will be presented by capital letters.

In this contribution the forward detector PLA is only used for trigger purposes, *i.e.* it defined central, intermediate and peripheral collisions by means of the selected particle multiplicity n_{PLA} . Minimum bias collisions correspond to no trigger selection, *i.e.* all multiplicities are accepted.

In the following sections we present results on

- the pion multiplicity n_π as function of the participants A_{part} ,
- the pion phase space distributions,
- the identification of Baryon($S = 0$) resonances in the (p, π^\pm) channel.

2. Charged pion multiplicities

The number of participants A_{part} is not directly measurable but has to be deduced from other observables x . For x one may choose any quantity which is a monotonous function of the impact parameter b , like the forward particle multiplicity n_{PLA} , or the total particle multiplicity n_{TOT} , or the baryonic charge $Z_{\text{CDC}}^{\text{bar}}$ measured with the CDC. The method to relate x with b and then A_{part} is to compare the measured cross section $\sigma(x)$ with the calculated cross section $\sigma_{\text{geo}}(b) = 2\pi \int_b^{b_{\text{max}}} \rho^2(r/2) r dr / \rho_0^2$, and then to obtain A_{part} from the geometrical and b dependent overlap of 2 identical nuclei with Saxon-Woods density profile $\rho(r) = \rho_0(1 + \exp\{(r - r_0)/a\})^{-1}$. In accordance with electron scattering we chose for the nuclear radius $r_0 = 1.2 \cdot A^{1/3}$, and for the surface parameter $a = 1.0 \pm 0.6 \text{ fm}$. The error in a was used to obtain an estimate for the uncertainty in determining A_{part} . The π^\pm multiplicities are shown in Fig. 1 as functions of A_{part} for the Au 1(left) and Ni 1(right) reactions. The π^- multiplicity as function of A_{part} was studied

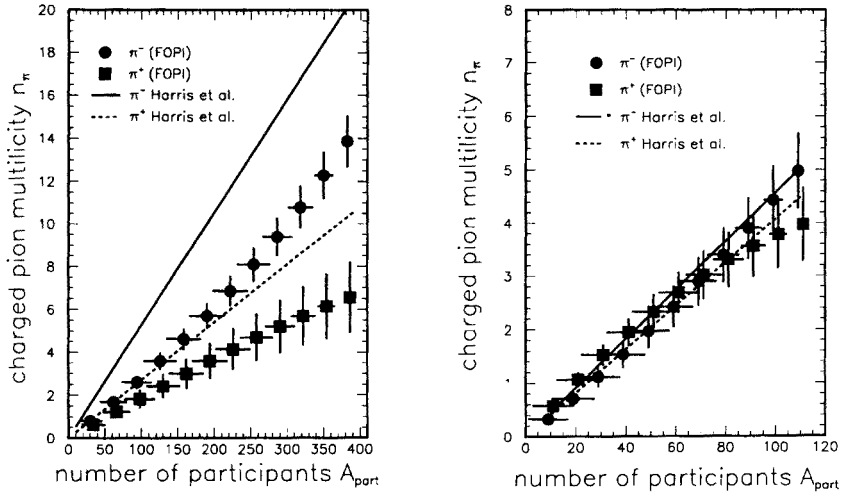


Fig.1. Pion multiplicities as functions of A_{part} for the reactions Au 1 (left) and Ni 1 (right).

previously by Harris *et al.* [1] in the light systems Ar + Ca and La + La. These results, when extrapolated to the Au 1 and Ni 1 reactions, are shown as straight lines in Fig. 1. Two conclusions are obvious: The number of charged pions n_π increases with A_{part} , and the data are in close agreement with the Harris extrapolation for the Ni 1, and also the Ni 2, Ni 3 reactions, but they are smaller than predicted by the Harris extrapolation in case of the Au 1 reaction. The observed reduction of the pion multiplicities in this reaction was also observed by the KaoS and TAPS collaborations [2].

To obtain the total pion yield per A_{part} the nonlinearities with A_{part} have to be taken into account. From $n_\pi = a_1 \cdot A_{\text{part}} + a_2 \cdot A_{\text{part}}^2 + a_3 \cdot A_{\text{part}}^3$ it follows that $\frac{\langle n_\pi \rangle}{\langle A_{\text{part}} \rangle} = a_1 + \frac{a_2}{2} \cdot A_0 + \frac{a_3}{3} \cdot A_0^2$, where A_0 is the total number of nucleons in the system. The results, obtained with the FOPI detector, are plotted in Fig. 2, the π^0 contribution was included using the isobar model [3].

The nonlinearities with A_{part} also influence the π^- to π^+ ratio R_π . If these ratios are normalized to the values expected from the isobar model, *i.e.* $R_\pi = 1.95$ for Au + Au and $R_\pi = 1.12$ for Ni + Ni, the increase of the normalized ratios with increasing A_{part}/A_0 is similar for all reactions studied, as shown in Fig. 3.

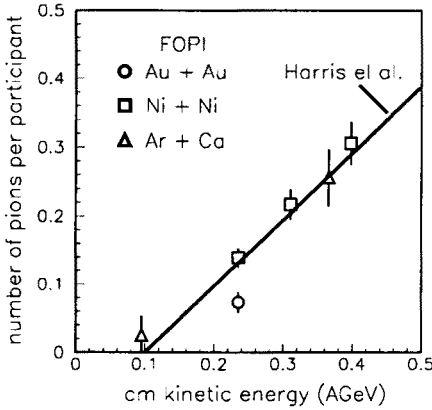


Fig.2

Fig.2. Pion production probability for different systems as function of energy.

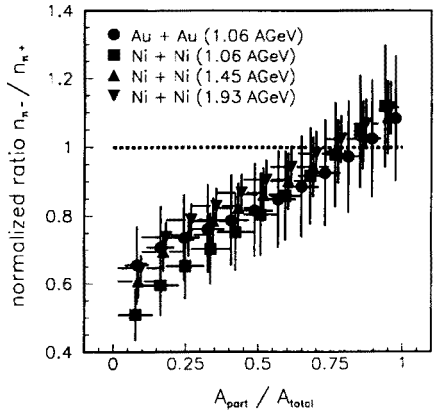


Fig.3

Fig.3. π^- to π^+ ratio for different systems as function of A_{part} .

3. The pion phase space distributions

The phase space distributions of charged pions under minimum bias condition are shown in Fig. 4 for the Ni 1 reaction. Increasing grey shades correspond to the increase of the invariant cross section $\frac{1}{p_t} \cdot \frac{d^2\sigma}{dp_t dy}$ on a logarithmic scale. A close inspection reveals that the phase space distributions

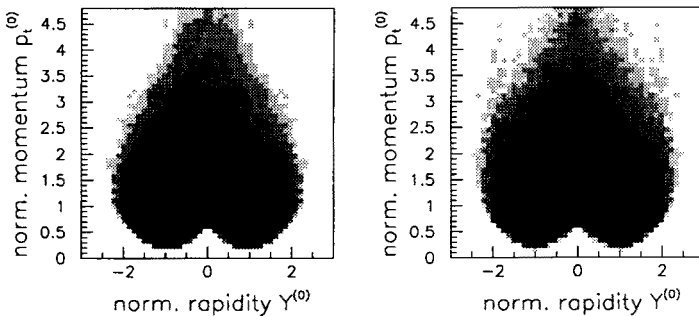


Fig.4. Phase space distributions of negative (left) and positive (right) pions.

are non-thermal. We have chosen to demonstrate this behaviour by projecting from the phase space distributions into the pion angular distributions $d\sigma/d\Omega$, the pion kinetic energies for different cm angles Θ , and into the pion rapidities with $p_t^{(0)} > 1$ in case of Au + Au and $p_t^{(0)} > 0.8$ in case of Ni + Ni collisions.

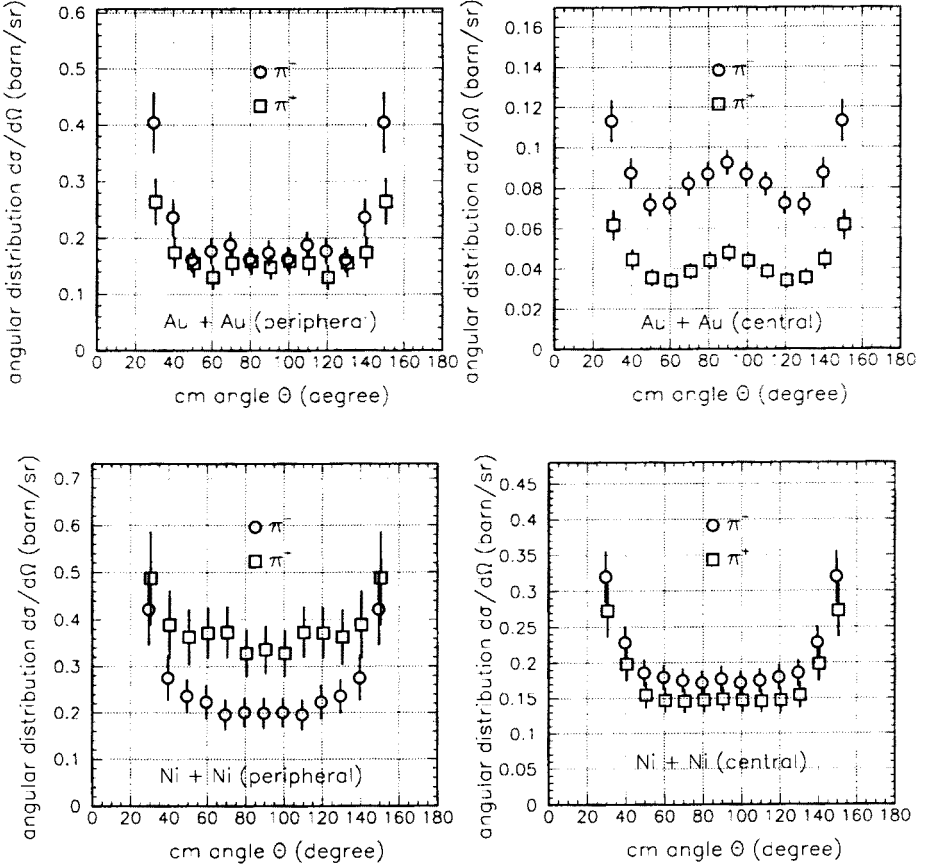


Fig.5. Pion angular distributions for the Au 1(top) and Ni 1(bottom) systems.

3.1. The angular distributions

The angular distributions $d\sigma/d\Omega$ of charged pions are non-isotropic, they display an enhancement at forward and backward angles as demonstrated in Fig. 5. The forward-backward peaking is predicted by the IQMD model, it is caused by the decay of Baryon resonances in the spectator matter which were excited by the absorption of pions from the participant. Contrary to the IQMD prediction the angular anisotropy does not decrease with decreasing impact parameter b : it is for central collisions ($A_{\text{part}}/A_0 > 0.9$) almost as strong as for peripheral collisions ($A_{\text{part}}/A_0 < 0.2$). It is possible that besides rescattering phenomena in the spectators also the known strong forward-backward enhancement of the fundamental $pp \rightarrow \Delta p$ process causes the observed anisotropies [3]. Furthermore the angular distributions

show a secondary maximum at $\Theta = 90^\circ$ in central collisions of the Au + Au system which is not apparent in the Ni + Ni system at the same conditions. At the moment the reason for this difference is not known.

3.2. The kinetic energies

In all reactions studied the shape of the kinetic energy spectra

$$\frac{1}{p_t E} \cdot \frac{d^2 \sigma}{dE d\Omega}$$

is concave, suggesting that the assumption of 2 temperatures, $T_{l,\pi}$ and $T_{h,\pi}$ has to be made if these spectra are to be fitted by exponentials. The deduced temperatures vary for angles $|90^\circ - \Theta| > 45^\circ$ whereas for angles around $\Theta = 90^\circ$ the temperatures remain reasonably constant. The average temperatures in this angular range are listed in Table I together with their contribution to the complete $\frac{d\sigma}{dE}$ spectrum. It is evident that the temperatures are almost independent of system mass or energy, whereas the relative contribution of the high-temperature component increases with system mass and energy.

TABLE I

Temperatures T and yields $R_T = \frac{I(T_l)}{I(T_h)}$ from fits to the pion energy spectra

	T_{l,π^-}	T_{l,π^+}	$T_{l,\pi}$	$R_T(\pi^-)$	$R_T(\pi^+)$
Au 1	42.2 ± 2.7	49.4 ± 2.3	96.4 ± 5.1	0.74 ± 0.28	0.75 ± 0.43
Ni 1	47.8 ± 1.3	52.5 ± 4.3	93.1 ± 6.6	1.54 ± 0.57	1.40 ± 0.98
Ni 2	51.7 ± 2.4	56.4 ± 2.7	99.5 ± 4.0	1.17 ± 0.63	1.53 ± 0.67
Ni 3	49.0 ± 1.0	56.6 ± 2.5	101.6 ± 2.0	0.52 ± 0.18	0.53 ± 0.14

3.3. The rapidity distributions

The projected rapidity distributions $\frac{d\sigma}{dY^{(0)}}$ of the Au 1 reaction are shown in Fig. 6 under minimum bias condition. The dotted curve displays the expected distribution if the pions were emitted from thermal sources at midrapidity, which have 2 temperatures $T_{l,\pi}$, $T_{h,\pi}$. The data deviate from these expectations and suggest that pion emission is enhanced at rapidities $|Y^{(0)}| > 1$. This finding is corroborated by the pion angular distributions which are enhanced at forward and backward angles in the cm frame. The Ni + Ni reactions yield similar results. The rapidity spectra were fitted by 3 Gaussians centered at $Y^{(0)} = 0$ and $|Y^{(0)}| = 1$, the latter representing the contributions of pions rescattered from target and projectile spectators.

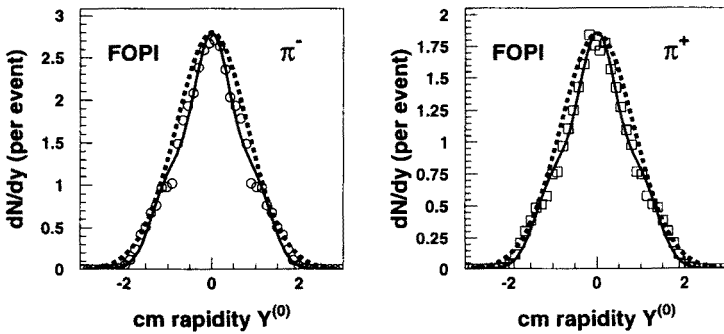


Fig.6. Au 1 rapidity distributions of negative (left) and positive (right) pions.

The relative contribution R_Y of pions from the participant region to pions from the spectator regions is displayed in Fig. 7. For the Ni + Ni reactions R_Y does not depend strongly on the impact parameter b , but it increases with energy. This is mainly due to an increase of the width of $\frac{d\sigma}{dY^{(0)}}|_{y=0}$, whereas the rapidity widths of pions from the spectators remain constant.

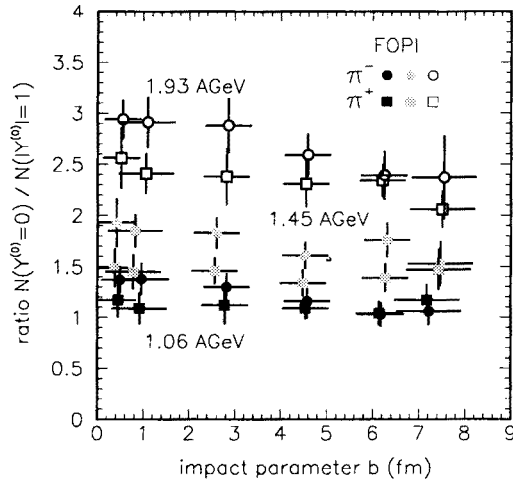


Fig.7. Impact parameter dependence of the ratio R_Y for Ni + Ni reactions

4. The identification of baryon resonances

Pions are assumed to originate from Baryon resonances which were excited by the nucleon-nucleon collisions in the participant. The $\Delta(1232)$ resonance dominates this process:



The observed independence of the pion temperature $T_{l,\pi}$ from system mass and energy supports this hypothesis. The concave shapes of the pion kinetic energy spectra, which is equivalent to the existence of a second higher temperature $T_{h,\pi}$, is interpreted as due to the emission of 'direct' pions or the contribution from higher Baryon resonances.

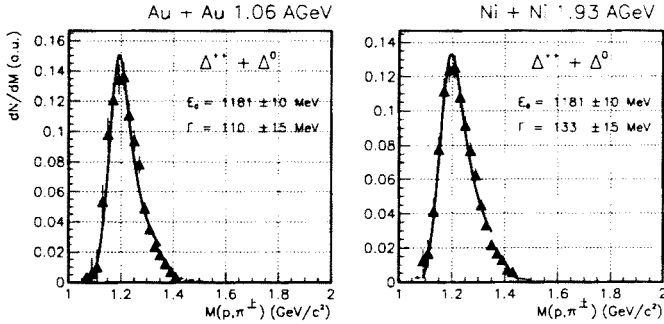


Fig.8. Invariant mass spectrum of (p, π) pairs with pion transverse momenta $100 < p_t < 200$ MeV/c for Au 1 (left) and Ni 3 (right) reactions.

The transient existence of Baryon resonances in the participant ought to be seen in the invariant mass spectra of correlated (p, π^\pm) pairs. Because of the large amount of uncorrelated protons, the probability to find a correlated pair amounts to $r = \frac{1}{n_p} \alpha \varepsilon_p \varepsilon_f \approx 0.01$, where n_p is the proton multiplicity, α accounts for isospin conservation, ε_p is the detector acceptance for protons, and ε_f takes care of the rescattering of protons by nuclear matter. The background of uncorrelated pairs S_b , which amounts to approximately 99% of all pairs S_t , is reconstructed using the technique of event mixing.

The invariant mass spectrum of the Baryon resonances is obtained from

$$S = S_t - (1 - r) \cdot S_b,$$

with ε_f as a free parameter. All p, π correlations other than those due to the resonance decay, are assumed to be of identical strength in S_t and S_b , in order to make this procedure applicable. For this purpose the azimuthal angle is measured with respect to the reaction plane, and only those events are mixed which have the identical n_p values. The effects caused by the pion rescattering in spectator matter are not well understood.

The background corrected invariant mass spectrum of (p, π^\pm) pairs depends on the pion transverse momentum p_t . It is shown for the Au 1 and Ni 3 reactions in Fig. 8 where $100 < p_t < 200$ MeV/c. The curves show the fitted Cugnon [4] parametrization of the Δ resonance, which yields a value for the Δ mass which is lower than accepted for the free Δ resonance.

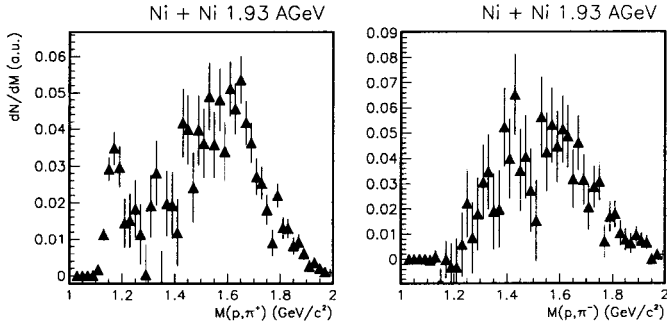


Fig.9. Invariant mass spectrum of (p, π^+) (left) and (p, π^-) (right) pairs with pion transverse momenta $400 < p_t < 600 \text{ MeV}/c$ for Ni 3 reactions.

Notice that (p, π^-) and (p, π^+) pairs were combined in Fig. 8. The Fig. 9 displays the invariant mass spectra separately for (p, π^-) and (p, π^+) pairs from the Ni 3 reaction where now $400 < p_t < 600 \text{ MeV}/c$. The spectra are shifted to larger mass values and they are different for the two types of pairs. This difference is expected when higher Baryon resonances become involved, since the (p, π^+) channel can only be populated by the decay of the Δ resonances, whereas the (p, π^-) channel can also be populated by the decay of N^* resonances.

5. Conclusion

The main conclusions from our investigation of the π^\pm production at 1 to 2 AGeV energy are:

The number of pions n_π per participants A_{part} is for the system Ni + Ni in agreement with the earlier results from Harris *et al.* [1], which were obtained with systems of total mass $A_0 < 200$. For the Au + Au system with $A_0 \approx 400$ the $\frac{\langle n_\pi \rangle}{\langle A_{\text{part}} \rangle}$ value is reduced by a factor 0.65 when compared to the results of Harris *et al.* The pions from the Ni + Ni and Au + Au systems are rescattered by spectator matter. This and the forward-backward enhancement of the fundamental $pp \rightarrow \Delta p$ process cause the pion rapidity distributions to become non-thermal. The concave shape of the pion kinetic energy spectra near midrapidity is generated by the decay of Baryon resonances. The contribution of resonances with masses larger than $\Delta(1232)$ increases with the pion transverse momentum, and also with the system energy. Equivalently high-energy pions become more abundant without a considerable change of the apparent pion temperature.

This work was supported by the Bundesministerium für Bildung und Forschung under contract no. 06 HD 525I (3), and by the Gesellschaft für Schwerionenforschung mbH under contract no. HDPEK.

REFERENCES

- [1] J.W. Harris *et al.*, *Phys. Rev. Lett.* **58**, 463 (1987).
- [2] P. Senger in *Multiparticle Correlations and Nuclear Reactions*, ed. J. Aichelin and D. Ardouin (World Scientific, 1988).
- [3] R. Stock, *Phys. Rep.* **135**, 259 (1986).
- [4] J. Cugnon and M. Lemaire, *Nucl. Phys.* **A489**, 781 (1988).